

## Monitoring microbial sulfate reduction in porous media using multipurpose electrodes

Chi Zhang,<sup>1</sup> Dimitrios Ntarlagiannis,<sup>1</sup> Lee Slater,<sup>1</sup> and Rory Doherty<sup>2</sup>

Received 16 September 2009; revised 10 March 2010; accepted 25 March 2010; published 21 July 2010.

[1] There is growing interest in the application of electrode-based measurements for monitoring microbial processes in the Earth using biogeophysical methods. In this study, reactive electrode measurements were combined to electrical geophysical measurements during microbial sulfate reduction occurring in a column of silica beads saturated with natural river water. Electrode potential (EP), self potential (SP) and complex conductivity signals were recorded using a dual electrode design (Ag/AgCl metal as sensing/EP electrode, Ag/AgCl metal in KCl gel as reference/SP electrode). Open-circuit potentials, representing the tendency for electrochemical reactions to occur on the electrode surfaces, were recorded between sensing/EP electrode and reference/SP electrode and showed significant spatiotemporal variability associated with microbial activity. The dual electrode design isolates the microbial driven sulfide reactions to the sensing electrode and permits removal of any SP signal from the EP measurement. Based on the known sensitivity of a Ag electrode to dissolved sulfide, we interpret EP signals exceeding 550 mV recorded in this experiment in terms of bisulfide ( $\text{HS}^-$ ) concentration near multiple sensing electrodes. Complex conductivity measurements capture an imaginary conductivity ( $\sigma''$ ) signal interpreted as the response of microbial growth and biomass formation in the column. Our results suggest that the implementation of multipurpose electrodes, combining reactive measurements with electrical geophysical measurements, could improve efforts to monitor microbial processes in the Earth using electrodes.

**Citation:** Zhang, C., D. Ntarlagiannis, L. Slater, and R. Doherty (2010), Monitoring microbial sulfate reduction in porous media using multipurpose electrodes, *J. Geophys. Res.*, 115, G00G09, doi:10.1029/2009JG001157.

### 1. Introduction

[2] Biogeophysics is a rapidly evolving Earth science discipline concerned with the links between dynamic subsurface microbial processes, microbial-induced alterations to geologic materials, and geophysical signatures [Atekwana and Slater, 2009]. There is growing interest in applying electrical geophysical techniques (resistivity, complex conductivity, and self potential (SP)) for biogeophysical projects as they have repeatedly been shown to be sensitive to bacterial cells, microbial growth and microbe-mineral alterations [Atekwana *et al.*, 2004a, 2004b; Naudet *et al.*, 2004; Personna *et al.*, 2008; Slater *et al.*, 2008]. Previous studies have confirmed the potential of electrical geophysics for characterizing microbial production of metabolic byproducts and resulting alteration of mineral surfaces [Werkema *et al.*, 2003; Atekwana *et al.*, 2004a, 2004b; Allen *et al.*, 2007; Che-Alota *et al.*, 2009], evaluating hydrological and bio-

transformations due to microbial reduction of heavy metals [Hubbard *et al.*, 2008; Williams *et al.*, 2009], improving understanding of metal and nutrient cycling driven by microbe-mineral transformations [Ntarlagiannis *et al.*, 2005b; Williams *et al.*, 2005; Personna *et al.*, 2008], and detection of microbes, microbial growth and biofilm formation [Abdel Aal *et al.*, 2004; Prodan *et al.*, 2004; Ntarlagiannis *et al.*, 2005a; Davis *et al.*, 2006; Abdel Aal *et al.*, 2009; Ntarlagiannis and Ferguson, 2009; Slater *et al.*, 2009].

[3] Biogeophysical signals are inherently non-unique, as complex and coupled biogeochemical processes alter subsurface physical properties in many ways and can drive multiple geophysical signatures over a wide range of spatial and temporal scales [Atekwana and Slater, 2009]. Additional biological, chemical, and physical information is typically required to reliably constrain interpretation of biogeophysical signals. One approach to constrain the interpretation is to simultaneously collect and analyze multiple electrical geophysical measurements (e.g., joint acquisition of complex conductivity and SP), along with any available aqueous geochemistry data (e.g., pH, Eh, and ion concentration). However, direct sampling of aqueous geochemistry is invasive, time consuming and expensive. Real-time monitoring of aqueous geochemistry using novel sensors offers promise in capturing temporal evolution of biogeochemical processes [Taillefert

<sup>1</sup>Department of Earth and Environmental Sciences, Rutgers, State University of New Jersey, Newark, New Jersey, USA.

<sup>2</sup>Environmental Engineering Research Centre, School of Planning, Architecture and Civil Engineering, Queen's University of Belfast, Belfast, UK.

*et al.*, 2000; *Viollier et al.*, 2003], but is usually impractical and cost-prohibitive to perform at high sampling density over large spatial domains.

[4] Recent studies have shown that electrodic potential (EP) measurements, using simple in construction and inexpensive electrodes, can be utilized to capture temporal and spatial variability in sulfide chemistry associated with microbial sulfate reduction under anaerobic conditions [*Williams et al.*, 2007; *Personna et al.*, 2008; *Slater et al.*, 2008]. The EP measurements record the tendency for spontaneous redox reactions to occur on the surfaces of metal and/or metal-metal salt electrodes. *Williams et al.* [2007], *Personna et al.* [2008] and *Slater et al.* [2008] showed that, in the presence of a bisulfide ( $\text{HS}^-$ ) concentration gradient across two Ag-AgCl metal electrodes, a galvanic cell (GC) potential is recorded, being the potential of an electrochemical cell with a known reactivity between the target compound and the electrodes used. We stress here that this EP method may provide only an approximation of  $\text{HS}^-$  concentration, as the accurate interpretation of  $\text{HS}^-$  may be limited due to possible complex electrochemical reactions in the system. More precise and diagnostic reactive electrode-based techniques, such as voltammetry, have been used with great success to determine chemical speciation associated with sulfide redox chemistry in the deep-sea [*Luther et al.*, 2001]. However, the anode and cathode in EP measurements are physically separated, and rely on very simple in construction and inexpensive electrodes that could potentially be deployed over large distances to provide spatially rich data sets collected in tandem with geophysical data sets.

[5] In this paper, we investigate the application of simultaneous EP/electrical geophysical measurements for monitoring microbial sulfate reduction. Unlike earlier studies [*Williams et al.*, 2007; *Personna et al.*, 2008; *Slater et al.*, 2008], we employ a dual electrode (Ag-AgCl metal as sensing/EP electrode; Ag-AgCl metal in KCl gel as reference/SP electrode) technique that constrains EP interpretation of  $\text{HS}^-$  concentration by using a non polarizing (SP) electrode as the reference cathode. This dual electrode strategy results in EP measurements with a constant stable reference potential, facilitating  $\text{HS}^-$  concentration predictions at the active electrode locations. In addition, this approach overcomes the overlooked limitations of earlier studies in that EP signals would be in error in the presence of significant SP signals, as have been repeatedly postulated to result from microbial activity [*Naudet et al.*, 2003, 2004; *Minsley et al.*, 2007; *Ntarlagiannis et al.*, 2007]. Finally, we demonstrate how complex conductivity, SP, and EP measurements can be jointly recorded in order to improve the understanding of microbial processes relative to electrical geophysical measurements alone.

[6] We describe a column experiment where EP, SP, complex conductivity, and resistivity measurements were made during microbial sulfate reduction in a column of silica beads saturated with natural river water amended with lactate. We show how EP measurements using geophysical instrumentation capture spatiotemporal evolution of sulfide production driven by the microbial activity. We also record a complex conductivity response consistent with previous studies [*Davis et al.*, 2006], further supporting the concept that complex conductivity can be used as a non-invasive

indicator of microbial growth and biomass formation in porous media, even in silica beads and in the absence of biodegradation. We discuss how the simultaneous collection of EP and complex conductivity data helps to better understand the processes in our microbial active system.

## 2. Experimental Methods

### 2.1. Electrodic Potential Measurements

[7] Point electrodes are commonly used for electrochemical applications to measure geochemical parameters, such as Eh and pH, as well as specific chemical concentrations (e.g.,  $\text{Br}^-$  using a bromide specific electrode). An open-circuit potential difference (high input impedance of the recording device impedes significant current flow) is recorded between a metal electrode in contact with the pore-filling electrolyte and a reference electrode in close proximity and connected to the metal electrode by a salt bridge. These open circuit potentials represent the tendency for an electrochemical (galvanic cell) reaction, associated with reactive compounds at the metal electrode, to proceed. A common target of such point electrodes is sulfide concentration, which can be estimated using Ag-Ag<sub>2</sub>S electrodes [*Berner*, 1963; *Mirna*, 1971; *Whitfield*, 1971; *Revsbech et al.*, 1983]. *Williams et al.* [2007], *Personna et al.* [2008], and *Slater et al.* [2008] showed how a pair of physically separated Ag-AgCl metal electrodes, as used in biogeophysical measurements, similarly record an open circuit potential between two points in a porous medium when the electrodes straddle a microbe-induced gradient in  $\text{HS}^-$  concentration. Being a simple approach, the EP measurements have inherent uncertainties discussed later, and are unlikely to give precise estimates of  $\text{HS}^-$  concentration. However, *Williams et al.* [2007] did show a positive correlation between sulfide concentration and measured EP response, supporting the concept of using these simple in construction and inexpensive electrodes, physically spaced over large distances, to capture spatiotemporal variability in  $\text{HS}^-$  concentration.

[8] Here we modify the EP method to improve (relative to prior EP studies) monitoring of spatiotemporal variations in microbial-driven aqueous sulfide chemistry. Similar to previous work, metal Ag-AgCl electrodes serve as sensing electrodes (anodic reaction). However, we use a non-polarizing (Ag-AgCl metal in KCl gel) electrode as reference electrode, such that the cathodic reaction occurs under known chemical conditions. The reference electrode therefore maintains a constant potential that is independent of changes in fluid properties in the column. The approach is therefore more akin to the measurement obtained with a point electrode (Figure 1b), except that the active electrode is distant from the reference electrode, and multiple active electrodes can be referenced to a single reference (Figure 1a). The assumed cathodic and anodic reactions, as well as overall galvanic cell reactions are summarized in Table 1, along with the individual standard potentials calculated from standard free energies of formation [*Stumm and Morgan*, 1996].

### 2.2. Complex Conductivity

[9] Complex conductivity measures the frequency ( $\omega$ ) dependent electrical behavior of a sample (e.g., a porous

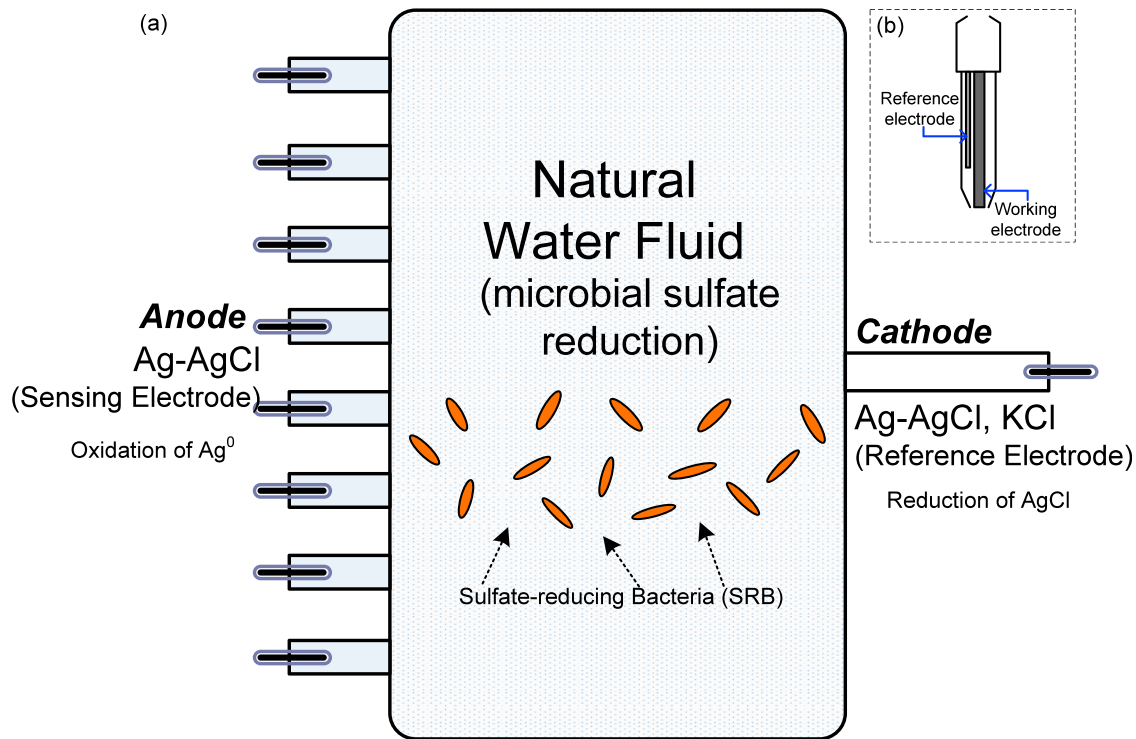


**Figure 1.** (a) In the column, sulfate-reducing bacteria (SRB) utilize sulfate as electron acceptor, reducing it to  $\text{HS}^-$ , while organic molecules (such as lactate) are used as the carbon source and oxidized to acetate. The Ag-AgCl in KCl gel (SP) electrode serves as a reference electrode whereby a cathodic reaction involves the reduction of AgCl coating. The anodic reaction at the sensing Ag-AgCl (EP) electrode is an oxidation of  $\text{Ag}^0$  as a result of a reaction with sulfide. The EP/SP electrode pair serves as a redox probe sensitive to  $\text{HS}^-$  concentration. (b) The dashed frame area represents a simple schematic of point electrode used in electrochemical-based techniques for determination of aqueous ion concentration for comparison.

medium or a suspension of cells). The measured complex conductivity  $\sigma^*(\omega)$  of a sample can be expressed as

$$\sigma^*(\omega) = \sigma'(\omega) + i\sigma''(\omega) \quad (1)$$

where  $\sigma'$  is the measured real part of  $\sigma^*(\omega)$ , being the conduction (energy loss) term,  $\sigma''$  is the measured imaginary part of  $\sigma^*(\omega)$ , being the polarization (energy storage) term,

and  $i = \sqrt{-1}$ . At low frequencies ( $<1000$  Hz),  $\sigma^*(\omega)$  of a saturated porous material can be modeled as the sum of an electrolytic conductivity  $\sigma_{el}$  resulting from ohmic conduction within the interconnected pore space, combined with complex mechanisms ( $\sigma_{surf}^*$ ) associated with grain-fluid surfaces. Two electrochemical interfacial polarization mechanisms assumed to occur in porous media are (1) polarization of ions in the electrical double layer at the mineral-fluid interface, and (2) polarization resulting from differences

**Table 1.** Half-Cell Electrochemical Reactions and Standard Potentials on Cathode and Anode, and Overall Reactions and Standard Potential of the Galvanic Cell<sup>a</sup>

	Electrodes	Reaction	Standard Potential ( $E^0$ )
Cathode	Ag/AgCl, KCl (1M) (reference electrode)	$\text{AgCl}_{(s)} + e^- \leftrightarrow \text{Ag}_{(s)} + \text{Cl}^-$ (Reduction of AgCl)	0.222 V
Anode	Ag/AgCl (sensing electrode)	$2\text{Ag}_{(s)} + \text{HS}^- \leftrightarrow \text{Ag}_2\text{S}_{(s)} + \text{H}^+ + 2e^-$ (Oxidation of $\text{Ag}^0$ ); $2\text{Ag}_{(s)} + \text{H}_2\text{S}_{(aq)} \leftrightarrow \text{Ag}_2\text{S}_{(s)} + 2\text{H}^+ + 2e^-$ ( $E^0 = 0.036\text{V}$ ); <sup>b</sup> $2\text{Ag}_{(s)} + \text{S}^{2-} \leftrightarrow \text{Ag}_2\text{S}_{(s)} + 2e^-$ ( $E^0 = 0.69\text{V}$ ) <sup>b</sup>	0.273 V
Overall galvanic cell		$2\text{AgCl}_{(s)} + \text{HS}^- \leftrightarrow \text{Ag}_2\text{S}_{(s)} + \text{H}^+ + 2\text{Cl}^-$	0.495 V

<sup>a</sup>Reactions are thermodynamically favorable ( $E^0 > 0$ ), and standard potentials (versus standard hydrogen electrode) are calculated from standard free energies of formation at 25°C [Stumm and Morgan, 1996].

<sup>b</sup>Anodic reactions with other major possible sulfate reduction products ( $\text{H}_2\text{S}$  and  $\text{S}^{2-}$ ) and standard potentials for half-cell reactions are also provided, which are not the predicted reactions in our study.

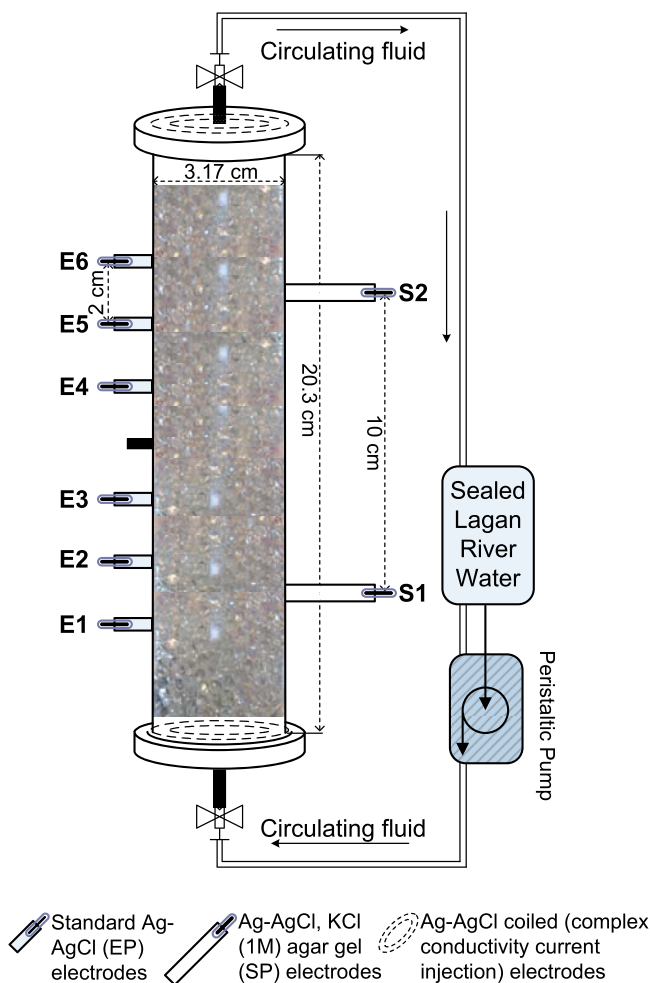


**Figure 2.** Schematic diagram of column setup showing flow through configuration, location of Ag-AgCl (EP) electrodes, Ag-AgCl in KCl gel (reference/SP) electrodes, and Ag-AgCl coil (complex conductivity current injection) electrodes. Lagan River water was pumped through the column via a peristaltic pump; pH and fluid conductivity ( $\sigma_f$ ) were monitored at the outflow.

in mobility of ions in the electrolyte driven by variable pore throat diameters.

[10] The sensitivity of complex conductivity measurements to subtle changes in the surface physical properties of geologic media makes it a suitable technique for investigating microbial growth and biofilm formation [Abdel Aal et al., 2004; Ntarlagiannis et al., 2005a; Abdel Aal et al., 2009; Slater et al., 2009], and detecting microbial growth and biomineralization transformations in porous media [Ntarlagiannis et al., 2005b; Williams et al., 2005; Personna et al., 2008].

### 2.3. Self Potential Method

[11] Self potential signals are voltages associated with a gradient in an electric field generated by internal current sources in the Earth. Self potentials are recorded using non-polarizing electrodes where both metallic electrodes are removed (by embedding in a gel or aqueous solution with identical chemistry at both metallic electrodes) from contact

with the pore fluids. This ensures that any potential recorded on the SP electrodes must result from internal current sources and not from galvanic potentials associated with reactions between compounds in the pore fluid and the metal electrodes.

[12] Self potential signals arise from multiple mechanisms. Streaming potentials are recorded in the presence of a streaming current source term resulting from the transport of excess charge in the electrical double layer at the solid-fluid interface of a porous medium in response to the viscous drag exerted by fluid flow through the pores. Streaming potentials have been employed with considerable success to monitor hydrological processes [Revil et al., 2002; Rizzo et al., 2004; Linde et al., 2007]. Another SP source mechanism is electrodiffusion, arising due to gradients in the chemical potentials of charge carriers. More important in biogeophysics research is the geobattery mechanism [Sato and Mooney, 1960]. Geo-batteries can develop when an electron conductor bridges electron donors and electron acceptors, resulting in current flow in response to the redox gradient (the thermodynamic driving force) [Sato and Mooney, 1960; Bigalke and Grabner, 1997]. Previous studies have suggested the potential for indirect detection of microbial activity from redox gradients produced using SP methods, with strong SP signals (+200 mV) observed at sites where microbial degradation of hydrocarbons is occurring [Nyquist and Corry, 2002; Naudet et al., 2003, 2004; Minsley et al., 2007].

## 3. Experimental Procedures

### 3.1. Sample Preparation and Column Setup

[13] The objective of our design was to capture EP and electrical geophysical signatures in response to sulfate reduction occurring in a porous medium composed of glass beads. We utilized two identical columns for this experiment; one was used as the experimental (biological active) column while the second served as a control. Lexan columns were constructed with inner diameter of 3.17 cm and a length of 20.3 cm. Both columns were dry packed with 3 mm glass beads (SiLibeads-Type M) with a measured porosity of  $0.38 \pm 0.02$  and density of  $2.5 \text{ kg/m}^3$ . Silica beads were chosen, in favor of quartzitic sand, since they offer high chemical resistance, excellent roundness, constant size and maintain the pore geometry before and after saturation by dry packing [Ntarlagiannis and Ferguson, 2009]. The experimental design is schematically illustrated in Figure 2.

[14] We used water from River Lagan (Belfast, Northern Ireland, UK) as the saturating fluid. The River Lagan, which feeds into Belfast Lough, is the recipient of numerous sewage and industrial discharges. The water sample contained suspended sediments and particles, known to contain sulfate-reducing bacteria (SRB) (K. P. Singh, Queen's University-Belfast, unpublished data, 2008). Chemical analysis of the collected river water involved ion chromatography (IC) and inductively coupled plasma mass spectrometry (ICP-MS) for the determination of major ions and metals, respectively. This analysis showed the water contains 29 mg/L  $\text{Cl}^-$ , 17 mg/L of  $\text{SO}_4^{2-}$ , 9.3 mg/L of  $\text{NO}_3^-$ , 0.60 mg/L of  $\text{PO}_4^{3-}$ , 0.40 mg/L of  $\text{NO}_2^-$ , 0.06 mg/L of  $\text{F}^-$ , 8.4  $\mu\text{g/L}$  of aqueous Cu, 7  $\mu\text{g/L}$  of aqueous Ni, Zn, and Cr, 5.8  $\mu\text{g/L}$  of aqueous Se, 0.7  $\mu\text{g/L}$  of aqueous As, and trace amounts of other metals. Two days prior to the experiment, the river water sample was spiked

with 2.24 g/L sodium lactate solution, and then placed in a dark airtight container to decrease oxygen penetration [Ramsing *et al.*, 1993] and promote SRB growth.

[15] The river water, amended with lactate to stimulate microbial growth, was used to saturate the experimental column. The control column was saturated with the same treated river water, but autoclaved to prevent biological activity. Both columns were positioned vertically and attached to separate closed circulation systems with 1L treated river water (experimental column) and 1L autoclaved treated river water (control column) respectively as the flow-through medium. A multichannel peristaltic pump was used to maintain a steady flow rate of  $\sim 2$  pore volumes/day ( $\sim 64$  ml/day) for both columns. All tubing and column components were sterilized before the experiment by autoclaving or rinsing with 70% ethanol to minimize contamination.

### 3.2. Electrode Potential and Self-Potential Measurements

[16] The experiment was performed at room temperature for a period of  $\sim 22$  days, although measurements for Days 10–18 were lost as a result of hardware problems. Measurements on the control column started with a two-day delay relative to the active column.

[17] The EP measurements were recorded on six metal Ag-AgCl electrodes installed in electrolyte filled chambers, in electrolytic contact with the column, placed 2 cm apart along one column side (Figure 2). These Ag-AgCl electrodes were made from high grade Ag wire (99.999%) that was immersed in a strong chlorine solution (6.5% NaOCl) until a continuous solid gray AgCl coating formed on the Ag surface. The SP signals were recorded using electrodes placed on the other side of each column, one of which also served as the reference electrode for the EP measurements (Figure 2). These electrodes were constructed by immersing a single Ag-AgCl metal electrode into 1M KCl agar gel and housed in a 15 ml pipette tip. The agar gel was prepared by dissolving 14 g/L agar powder and 74.5 g/L KCl into heated DI water. The solution was then stirred until it became clear, when 0.27 g/L HgCl<sub>2</sub> of biocide was added to inhibit the erosion of agar gel by microbes. The final solution was left to cool in the pipette tips. The fine open end of the pipette tip ensured electrolytic contact between the electrode and the electrolyte in the column.

[18] The EP and SP measurements were obtained with a high-impedance ( $>10$  Mohm  $\pm 1\%$ ) Keithley 2701 digital multimeter (DMM) data logging system. We collected measurement every 15 min during the experimental period, with the exception of 30-min intervals when complex conductivity measurements were performed. For all measurements we use the same reference electrode, S1 (Figure 2). The EP measurements were recorded between S1 and E1, E3, E4, and E6, whereas SP measurements were recorded between S1 and S2. In both EP and SP measurements the reference electrode was connected to the negative terminal of the digital multimeter by convention.

### 3.3. Complex Conductivity Measurements

[19] Complex conductivity measurements were obtained daily (from Day 0 to Day 10) with a two-channel dynamic

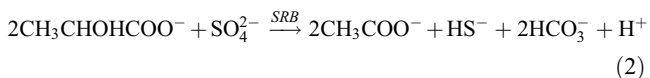
signal analyzer (DSA, National Instrument 4551) for frequencies between 0.1 and 1000 Hz at 40 logarithmic intervals [Slater and Lesmes, 2002]. The commonly used four-electrode configuration technique was utilized; two coiled Ag-AgCl electrodes located at each end of the column were used for current injection (Figure 2). The resulting potential was recorded between SP electrode pair S1 and S2. The magnitude ( $|\sigma|$ ) and the phase shift ( $\varphi$ ) were measured relative to a known high precision resistor on channel 1. The real ( $\sigma' = |\sigma| \cos \varphi$ ) and imaginary ( $\sigma'' = |\sigma| \sin \varphi$ ) components of the sample complex conductivity were then calculated. The instrumentation and setup applied in this study is similar to previous studies [Ntarlagiannis *et al.*, 2005a], with phase accuracy of  $\sim 0.06$  mrad.

### 3.4. Sampling and Geochemical Analysis

[20] Aqueous geochemical measurements of fluid conductivity ( $\sigma_f$ ), Eh, and pH of circulating fluid were taken daily for both experimental (from Day 1) and control columns (from Day 4). A 1.5 ml fluid sample was extracted and anaerobically sealed using a sterile syringe inserted into the tubing, and Eh/pH point probes was immediately immersed in fluid to minimize the contact of sample and ambient air. The  $\sigma_f$  was subsequently measured using a conductivity probe. We chose not to determine sulfide concentrations (e.g., colorimetrically) in this experiment because of potential sampling errors from a closed anaerobic system of limited volume. Sulfide is unstable and easily chemically oxidized under aerobic conditions, leading to sulfate production. In addition, previous studies have already proven the positive correlation between measured EP response and sulfide concentration [Williams *et al.*, 2007] as we discussed in Section 2.1, and this was not our objective here.

### 3.5. Bisulfide Concentration Estimation From EP

[21] The SRB can utilize H<sub>2</sub> and/or low molecular weight organic matter (e.g., lactate and pyruvate) as an electron donor and sulfate as an electron acceptor under anaerobic conditions while producing sulfide [Maier *et al.*, 2000]. Taking lactate for instance, the reaction could be summarized in equation (2), whereby dissimilatory sulfate reduction by bacteria is the most kinetically favorable mechanism by which sulfide is produced [Ledin and Pedersen, 1996],



At circumneutral pH, HS<sup>-</sup> is the predominant sulfide species in aqueous system, although other major sulfide species are H<sub>2</sub>S and S<sup>2-</sup>. In our experiment with the presence of HS<sup>-</sup>, oxidation of silver occurs at the anode (metal Ag-AgCl electrode) along with the concurrent conversion of AgCl to Ag<sub>2</sub>S due to the much smaller stability constant ( $K_{\text{sp}}$ ) of Ag<sub>2</sub>S. Reduction of the AgCl electrode coating occurs at the non-polarizing reference electrode. The electrochemical reactions on the electrodes and the associated half-cell potentials are summarized in Table 1.



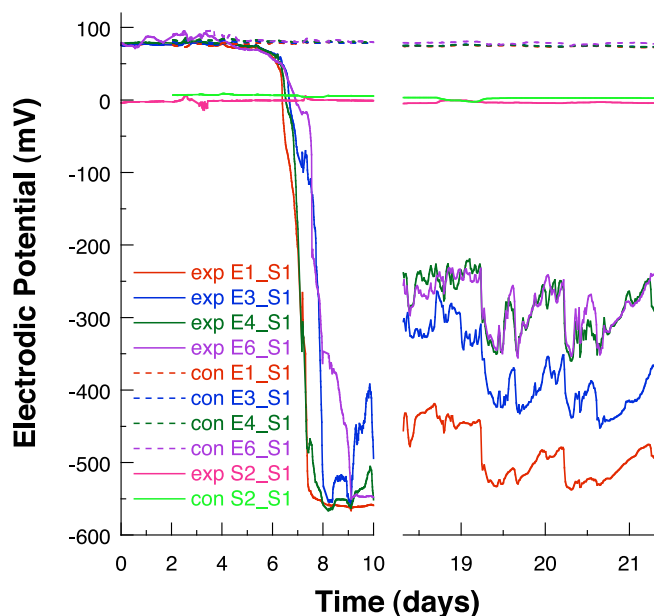


**Figure 3.** Electrode potential (EP) and self-potential (SP) measurements over the experiment duration. Solid color lines denote EP signals at different locations in experimental column referenced to S1, and color dashed lines indicate EP signals at the same locations in control column. Magenta and bright green lines show the SP signals at pair S2\_S1 in experimental and control column, respectively.

[22] Utilizing the Nernst equation, the  $\text{HS}^-$  concentration ( $[\text{HS}^-]$ ) can be estimated given EP and pH measurements from

$$\Delta E_{\text{cell}} = E_{\text{cell}}^0 - \frac{RT}{nF} \log \frac{[\text{H}^+][\text{Cl}^-]^2}{[\text{HS}^-]} \quad (3)$$

where  $E_{\text{cell}}^0$  is the standard potential of the overall galvanic cell reactions determined from two half-cell potentials (Table 1), and  $\Delta E_{\text{cell}}$  is the EP of our system. However, the potential recorded between the Ag-AgCl metal electrode and the reference electrode is actually the sum of the EP and any SP signal in the system (a fact that was overlooked in previous studies using EP [Williams *et al.*, 2007; Personna *et al.*, 2008; Slater *et al.*, 2008]). In our setup, the  $\Delta E_{\text{cell}}$  can be determined by subtracting any SP signal (as recorded between the non-polarizing electrodes S1 and S2 in Figure 2) from the total potential recorded between any EP electrode (E1-E6) and S1. The hydrogen concentration ( $[\text{H}^+]$ ) is known from pH, which was measured daily and linearly interpolated to predicted values at 15 min intervals (recording interval for EP measurements). As the chloride concentration ( $[\text{Cl}^-]$ ) is known (1M KCl in the cathode),  $[\text{HS}^-]$  is the only unknown in equation (3). It is important to emphasize that the  $[\text{HS}^-]$  calculated here is the localized concentration immediately adjacent to the sensing EP electrode, and it does not necessarily represent  $[\text{HS}^-]$  of the bulk

fluid. Furthermore, the approach is based on assumptions that we discuss in detail later.

## 4. Results

### 4.1. Visual Observation

[23] A darkening of the fluid in the column and tubing was visually observed, being first noted at the bottom of the column (inflow) (Figure 2) at Day 6, and covered the entire active column after Day 8. At the beginning of experiment, both aerobic and anaerobic microorganisms (including SRB) likely co-existed. The observed darkening is indicative of microbial sulfate reduction, expected as the river water contained a significant amount of sulfate (17 mg/L) and SRB communities. In the presence of available metal cations (e.g.,  $\text{Fe}^{2+}$ ,  $\text{Cu}^{2+}$ , and  $\text{Zn}^{2+}$ ),  $\text{S}^{2-}$ , the main product of sulfate reduction, binds to form insoluble metal sulfide precipitates (MeS). In our experiment the observed darkening was attributed to possible precipitation of such metal-sulfide compounds. The gradual transition from bottom to top may represent the higher availability of nutrients for SRB closer to the inflow. Alternatively, this darkening could also conceivably arise simply from the settling and/or filtration of MeS within the column. This visual evidence of SRB activity was backed up by the characteristic sulfurous smell noted during syringe extraction of fluid from the experimental column. In the control column no change of color or sulfurous smell was observed over the duration of the experiment, indicating no significant SRB activity as expected.

### 4.2. EP and SP Measurements

[24] Electrode potentials recorded at E1, E3, E4, and E6 on the experimental column relative to the reference electrode are shown in solid color lines in Figure 3. The measurements taken at the same pairs on the control column are also shown in Figure 3 in color dashed lines. At the beginning of experiment, steady ( $\sim 75$  mV) EP measurements were observed for both the experimental and control column until Day 6 when strong negative potentials in the experimental column developed. The EP readings in the control column (color dashed lines) remained the same thereafter, suggesting that no changes in redox state occurred in the natural waters in the absence of biological mediated redox reactions. In contrast, peak negative EP values ( $-550 \sim -560$  mV) were measured in the experimental column after Day 7 and were maintained until  $\sim$ Day 10. Between Day 19 (446 h) and the end of the experiment, the EP signals of all pairs in the experimental column slowly decreased in magnitude. During this time, the bottom electrode E1 (pair E1\_S1) showed the least change, followed by pair E3, with E4 and E6 behaving similarly and exhibiting the greatest decrease.

[25] Figure 3 also shows SP data at pair S2\_S1 for both experimental (magenta solid line) and control (bright green solid line) columns. The measurements were relatively steady ( $+3 \pm 4$  mV) for the duration of the experiment. The SP in the control column was slightly ( $\sim 5$  mV) higher than the SP in the experimental column.

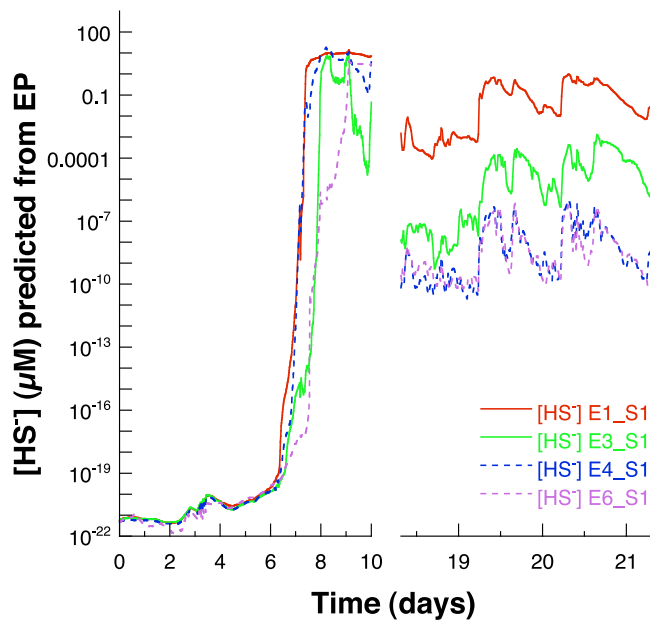


**Figure 4.** Estimated hydrogen sulfide concentration ( $[\text{HS}^-]$ ) at different locations in the experimental column over the experiment duration. The  $[\text{HS}^-]$  was determined by the Nernst equation as a function of theoretical cell potential ( $E_{\text{cell}}^0$ ), cell potential ( $\Delta E_{\text{cell}}$ , equivalent to measured EP corrected by eliminating SP), and pH, while holding  $[\text{Cl}^-]$  (1 M) and temperature ( $25^\circ\text{C}$ ) constant. The concentrations shown here are in  $\mu\text{M}$ .

#### 4.3. $\text{HS}^-$ Concentration

[26] The calculated  $[\text{HS}^-]$  (in  $\mu\text{M}$ ) in the experimental column is showed in Figure 4 for pairs E1\_S1, E3\_S1, E4\_S1, and E6\_S1. Reflecting the relative small increase in EP early in the experiment,  $[\text{HS}^-]$  slightly increased from Day 0 to Day 5, the response being nearly the same for each pair. Starting from Day 6,  $[\text{HS}^-]$  dramatically increased for all pairs. Pair E1\_S1 was the first to develop peak values ( $14.279 \mu\text{M}$ ), followed by pair E4\_S1 (peak value  $18.15 \mu\text{M}$ ), E3\_S1 (peak value  $9.96 \mu\text{M}$ ), and E6\_S1 ( $4.13 \mu\text{M}$ ). These peak values maintained a plateau from Day 7 to ~Day 10. During Day ~19 to Day 22,  $[\text{HS}^-]$  decreased, showing a gradual decline from pair E1\_S1 to E6\_S1. At the end of this experiment, pair E1\_S1 had the highest estimated  $[\text{HS}^-]$ , followed by pair E3\_S1, while pairs E4\_S1 and E6\_S1 had the lowest estimated concentration.

#### 4.4. Complex Conductivity and Fluid Conductivity

[27] The complex conductivity measured between electrode pair S1\_S2 from both columns was used to calculate  $\sigma'$  (Figure 5a) and  $\sigma''$  (Figure 5b) components, respectively (34 Hz values shown). The  $\sigma'$  (Figure 5a) increased from  $0.085 \text{ S/m}$  to  $0.27 \text{ S/m}$  from Day 0 to Day 4 and remained steady in the experimental column, while  $\sigma'$  remained at  $0.07 \text{ S/m}$  in the control column and showed no significant changes throughout the experiment. The  $\sigma''$  (Figure 5b) in the experimental column increased from  $1.16 \times 10^{-5} \text{ S/m}$  (Day 0) to  $4.29 \times 10^{-4} \text{ S/m}$  (Day 5), and then decreased to  $4.76 \times 10^{-5} \text{ S/m}$  on Day 10. The magnitude of the  $\sigma''$

response in the control column was constant at  $1.1 \times 10^{-5} \text{ S/m}$  over the duration of the experiment.

[28] Aqueous geochemical analysis of fluid samples showed  $\sigma_f$  in the experimental column was the same as in the control column at the beginning of experiment, but later increased to ~5 times higher than it in control column. The  $\sigma_f$  value remained steady at  $0.23 \text{ S/m}$  in the control column, whereas  $\sigma_f$  in the experimental column increased with slight fluctuations. Normalizing the real conductivity by fluid conductivity ( $\sigma'/\sigma_f$ ), resulted in a flat response, indicating that increases in  $\sigma'$  in the experimental column result from associated increases in  $\sigma_f$ .

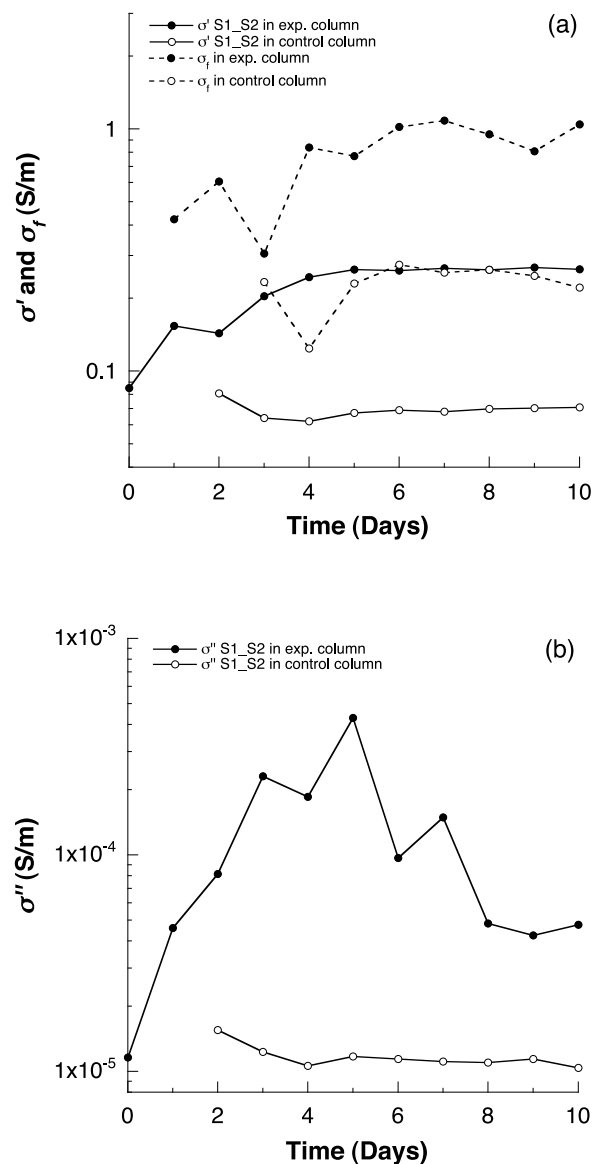


**Figure 5.** (a) Fluid conductivity  $\sigma_f$  (dashed lines) and results of measured real conductivity  $\sigma'$  (solid lines) for pair S1\_S2 in both experimental (closed black circles) and control (open circles) columns. (b) Imaginary conductivity ( $\sigma''$ ) for pair S1\_S2 in both experimental (closed black circles) and control (open circles) columns. Both  $\sigma'$  and  $\sigma''$  shown here are at 34 Hz from Day 0 to Day 10.

[29] The pH in the experimental column decreased from 7.81 to 7.29, and it dropped from 8.98 to 7.42 in control column throughout the experimental period. This drop was likely due to the existence of CO<sub>2</sub> and organic acids, generated from the degradation of complex organic material and biological respiration in the column, dissociated to form protons. The Eh (data not shown) recorded at the fluid sample varied considerably, probably reflecting problems with sampling and exposure to ambient air prior to Eh probe measurements.

## 5. Discussion

### 5.1. Sulfide Chemistry and Reactive Electrodes

[30] Our results show how microbial-driven sulfide chemistry can be monitored using EP measurements made on simple in construction and inexpensive metal electrodes, that can also be used to make electrical geophysical measurements. We note that the EP response curves recorded in this experiment are quite similar in shape and magnitude when compared to those previously recorded on other experiments using mixed SRB cultures [Slater *et al.*, 2008], as well as those recorded for a pure *D. vulgaris* culture [Personna *et al.*, 2008]. However, we do not expect identical EP responses across these systems as the mineral matrix, growth media and cultures differ significantly. These differences could result in different onsets of SRB activity (e.g., the EP response curves in the work by Slater *et al.* [2008] develop later than in this study) and differences in total sulfide produced. Although laboratory experiments using pure cultures are more easily quantifiable, they do not represent the real world. Our laboratory experiment suggests that we can bridge the gap between laboratory and field scale applications and this technology is transferable to the field scale.

[31] We recorded an open-circuit potential, as in previous work [Personna *et al.*, 2008; Slater *et al.*, 2008], which increases with the difference in HS<sup>-</sup> concentration between the cathode and anode. However, in our study we utilize two types of electrodes, allowing for the correction of any SP signals during the EP measurement. We note that the presence of conductive metals between S1 and S2 could facilitate a geobattery SP mechanism [Sato and Mooney, 1960; Bigalke and Grabner, 1997] within the column given a sufficient redox gradient between these two locations. Even though, we only observe very small SP signals (few mV in both columns), suggesting there is no apparent mechanism associated with this microbial sulfate reduction process that could generate current sources. This result is expected given that (1) the redox gradient between S1 and S2 is small in this closed circulation experiment, and (2) it is unlikely that the MeS precipitates were extensive enough to form continuous conduction paths.

[32] Instead, the SP signal probably represents the streaming potential due to the flow of the saturating fluid through the glass beads. In our case then, the SP correction needed to determine EP from the potentials recorded on the metal electrodes was minor. However, recent experiments suggest that this may not be the case in field-scale studies. Previous studies have identified large (+200 mV) SP readings, postulated to be due to biogeobatteries [Naudet *et al.*, 2003, 2004; Minsley *et al.*, 2007], in the presence of strong

microbial-driven redox potential gradients. In such field studies, it would be critical to remove the SP signals from the EP responses prior to estimation of sulfide concentration. The previous EP studies [Williams *et al.*, 2007; Slater *et al.*, 2008] employed only reactive metallic electrodes (Ag-AgCl electrodes), therefore making it impossible to determine the contribution of any SP signal to the potential recorded on the metallic electrodes. The fact that SP was not quantified in these earlier studies has implications for the accuracy of the estimated sulfide concentration and adopted interpretation of the mechanism driving the measured potentials in general.

[33] The use of a constant potential SP electrode in the EP measurement isolates the sulfide chemistry information to a single reactive electrode. In contrast, previous studies [Williams *et al.*, 2007; Personna *et al.*, 2008; Slater *et al.*, 2008] using two reactive electrodes being located in a stable/quiescent, non-reactive environment in order to be isolated from confounding effects of reactive fluid chemistry (e.g., on the column influent for flow-through experiments). The use of a constant potential SP electrode for the reference enhances our confidence in the possible quantitative estimation of HS<sup>-</sup> concentration at the anode, as the concentration at the cathode is known to be constant. Our approach requires a reference SP electrode (Ag-AgCl immersed in a KCl gel), where the electrodic reaction is fixed and known. When two reference electrodes are available, SP measurements can also be performed. These permit correction of the measurements made on metallic electrodes for SP signals and estimation of EP.

[34] Our approach to biogeophysics monitoring, couples electrical geophysical measurements with a simple measurement sensitive to pore fluid redox chemistry at the electrodes. The interpretation of biogeophysical signals is inherently uncertain due to the multiple possible sources for the recorded electrical signals; additional measurements, such as aqueous geochemistry measurements, are clearly advantageous for constraining the interpretation. In our experiment we demonstrate a quick and inexpensive means to capture spatial and temporal variability in microbial-driven sulfide chemistry using the same electrodes applied for the electrical geophysical measurements. Geophysical monitoring of microbial processes using large numbers of electrodes is increasingly being conducted [Daily and Ramirez, 1995; Werkema *et al.*, 2003; Atekwana *et al.*, 2004b; Allen *et al.*, 2007; Minsley *et al.*, 2007], and our approach could be adopted to determine variations in sulfide concentration at hundreds of locations as defined by the placement of electrodes. Such a sampling density would be prohibitively costly and invasive if on site extraction and sampling was conducted. The suggested EP electrode design is sensitive to other electrochemical reactive species and could be used as a qualitative Eh indicator in environments where no additional information is available; in certain cases where the chemistry is known and the dominant electrochemical species are identified or assumed (e.g., sulfide due to SRB activity in our experiment), EP measurements can be used to quantitatively estimate the concentration of the species of interest.

[35] The quantitative interpretation of the EP signals in terms of sulfide concentration is, however, based on a number of assumptions. First, we assume that the reactions



on the anode effectively alter the anode from Ag-AgCl to Ag-Ag<sub>2</sub>S, which is a thermodynamically favorable but unverified reaction here. Second, we treat this system as a single-potential system (although it is probably a mixed potential in reality), and we attribute the EP signals only to HS<sup>-</sup>, without accounting for any other possible sulfate reduction products in the sulfide family (e.g., SO<sub>3</sub><sup>2-</sup>, S<sup>2-</sup> ions, dissolved H<sub>2</sub>S, and etc.) or any transformation between different sulfide species. Third, we assume the reactions describe an ideal Nernstian response over the whole range of HS<sup>-</sup> concentrations. In fact, a linear Nernstian slope is only obtained for concentrations from 10<sup>-6</sup> to ~10<sup>-4</sup> mol/L of total sulfur, the range depending on pH and ion concentration of the aqueous solution [Revsbech *et al.*, 1983; Jeroschewski *et al.*, 1993; Lawrence *et al.*, 2000]. These problems are not unique to our system, but are recognized difficulties in using point Ag/Ag<sub>2</sub>S electrodes to determine sulfide. In addition to deviation from ideal Nernstian behavior, other problems include long response times and poisoning of the reference electrode [Jeroschewski *et al.*, 1996; Lawrence *et al.*, 2000].

[36] Despite these limitations, the Ag/Ag<sub>2</sub>S electrode has for a long time offered the only reasonable solution to estimate sulfide at high spatial resolution at the aerobic and anaerobic interface in aquatic sediments and biofilms, where distinct gradients of chemical and physical parameters exist [Revsbech *et al.*, 1986; Kühl and Jørgensen, 1992]. Electrode-based electrochemical determination of sulfide in aqueous system has a lower determination limit of a few ppb and an upper limit of hundreds of ppm, depending on the methods and electrodes [Lawrence *et al.*, 2000]. Sulfide concentration in environmental systems varies from a few ppb (e.g., in oxic seawater) to thousands of ppm (e.g., in pore waters from salt marshes). In the latter case, the use of simple in construction and inexpensive multipurpose electrodes, as proposed here, could conceivably capture spatiotemporal changes calibrated in terms of actual sulfide concentration. However, in many environments it will likely only be possible to use EP measurements to infer patterns of sulfide variation, but not quantify absolute concentrations.

[37] Even if the determination of HS<sup>-</sup> concentration is not entirely accurate in our system, the EP signals still capture the onset of SRB activity, along with spatiotemporal variability in the processes. Such information is very valuable from a monitoring standpoint, and can also improve understanding of biogeophysical signals associated with microbial processes. In fact, validation of field studies often requires accredited chemical and biological analysis techniques, and the application of EP potentially provides a cost effective real time monitoring method that could supplement expensive chemical and biological analysis. In future studies, the estimation of HS<sup>-</sup> using our approach might be improved by recording the real time temperature, pH, and ion concentration of the fluid, or constructing electrodes with a constant reactive area [Barrett *et al.*, 1988]. It may also be possible to calibrate these electrodes for variations in pH and ion concentration.

## 5.2. Electrical Geophysical Signals

[38] Our complex conductivity measurements revealed temporal increases in  $\sigma'$  in the experimental column resulting from increases in fluid conductivity (as supported by

normalizing the  $\sigma'$  data by  $\sigma_f$ ). Fluid conductivity is largely controlled by the total dissolved solids representing the number of ions present in the solution. Organic acids (acetic acid) produced as metabolic by-products of degradation of larger molecular organic matter (e.g., lactate) have been shown to cause mineral dissolution resulting in the release of ions into the pore space, thus increasing the conductivity of the pore fluid [Abdel Aal *et al.*, 2004; Allen *et al.*, 2007]. In addition, biomass and decay of bacterial cells may contribute to higher electrical conductivity [e.g., Slater *et al.*, 2009].

[39] More significantly, our complex conductivity measurements also reveal a  $\sigma''$  signal that is similar to that observed in work of Davis *et al.* [2006] and attributed to microbial growth/attachment followed by subsequent death/detachment. Given that no signals were observed in the control column, we are confident that the source is microbial in origin. The possible presence of metal-sulfide precipitates in the experimental column, which might be the reason for the observed darkening of fluid, cannot explain the  $\sigma''$  response, as  $\sigma''$  declined after reaching the peak value at Day 5. Although previous work has shown similar  $\sigma''$  curves that were attributed to changes in mineral aggregation and variation in the spatial position of sulfide-encrusted cells [Ntarlagiannis *et al.*, 2005b; Williams *et al.*, 2005], these studies were conducted on columns with continuous supply of metals. In contrast, any  $\sigma''$  response associated with metal-sulfide precipitates in our metal-limited system might be expected to show just the early time response observed in these previous studies, whereby  $\sigma''$  increases in response to dispersed metal precipitates. This is consistent with elevated  $\sigma''$  values throughout the experiment and dark fluid being observed until the end of experiment.

[40] We suggest that our  $\sigma''$  response in the experimental column reflects changes of microbial population in our system. Davis *et al.* [2006] showed a correlation between  $\sigma''$  and microbial growth in their diesel fuel and nutrient broth saturated sand column experiment. The model of Davis *et al.* [2006] seems plausible in our case, although our study was conducted under much simpler experimental conditions. More recently, Slater *et al.* [2009] demonstrated an electrical conductivity response exhibiting the characteristics of microbial growth models. Our results suggest that a signal associated with microbial growth/attachment to death/detachment cycle can be captured during microbial sulfate reduction in the absence of hydrocarbon biodegradation. In our experiment,  $\sigma''$  reached peak values at Day 5, although the largest EP signals developed on Day 6. This delay in the EP signals relative to the  $\sigma''$  peak may suggest that 1) sulfate reduction by SRB was not initiated until oxygen is depleted, and/or 2) significant time is needed for electrochemical conditions at the electrode to develop for EP signal generation. The microbial activity between Days 2–8 captured with  $\sigma''$  is likely the response of both aerobic and anaerobic microorganisms (including SRB) existing in the natural fluid. The peak in SRB activity occurred later as captured in the EP response. In this case,  $\sigma''$  detects the growth of all microbial cells in the column whereas the EP signals are associated only with SRB activity. Our work thus lends strength to the notion that the signal recorded in the work of Davis *et al.* [2006] is an important biogeophysical signal

that is not specific to the conditions of the *Davis et al.* [2006] experiment.

## 6. Conclusion

[41] Here we have shown how EP measurements, in conjunction with SP and complex conductivity measurements, can be used to monitor spatial and temporal variability in microbial sulfate reduction within a porous medium saturated with natural river water using dual electrode sensors. The dual electrode approach permits an SP correction to the EP measurement, and isolates the microbial driven sulfide chemistry to a sensing/EP electrode while holding the reference/SP electrode constant. We assume these open-circuit EP signals are associated with electrochemical reactions that occur on the Ag-AgCl (sensing/EP) electrode in the presence of dissolved sulfide, although it is possible that other microbial driven redox reactions may also have contributed to the observed signal. The HS<sup>-</sup> concentration near the EP electrode surface could be estimated from EP signals based on certain assumptions. Our complex conductivity results are consistent with previous biogeophysics research, showing sensitivity to microbial activity in porous media. Thus EP measurements using Ag-AgCl electrodes offer a simple approach to capture spatial variability in microbial driven sulfide chemistry that can be collected using the same instrumentation and hardware as used for electrical geophysics measurements. The joint use of EP and complex conductivity measurements could facilitate simultaneous monitoring of individual microbial communities (e.g., sulfate reducers), while also monitoring net microbial growth. Our work may lead to the application of multipurpose electrodes to improve the geophysical and geochemical monitoring in biogeophysics research.

[42] **Acknowledgments.** This work was performed at Queen's University Belfast, Belfast (UK) in the Environmental Engineering Research Center. This material is based upon work supported by the National Science Foundation under grant EAR-0433729. We thank Kushal P. Singh (Queen's University Belfast, Belfast, UK) for his assistance in laboratory work. Review comments provided by two reviewers and the Associate Editor significantly improved this manuscript.

## References

- Abdel Aal, G. Z., E. A. Atekwana, L. D. Slater, and E. A. Atekwana (2004), Effects of microbial processes on electrolytic and interfacial electrical properties of unconsolidated sediments, *Geophys. Res. Lett.*, *31*, L12505, doi:10.1029/2004GL020030.
- Abdel Aal, G., E. Atekwana, S. Radzikowski, and S. Rossbach (2009), Effect of bacterial adsorption on low frequency electrical properties of clean quartz sands and iron-oxide coated sands, *Geophys. Res. Lett.*, *36*, L04403, doi:10.1029/2008GL036196.
- Allen, J. P., E. A. Atekwana, E. A. Atekwana, J. W. Duris, D. D. Werkema, and S. Rossbach (2007), The microbial community structure in petroleum-contaminated sediments corresponds to geophysical signatures, *Appl. Environ. Microbiol.*, *73*(9), 2860–2870, doi:10.1128/AEM.01752-06.
- Atekwana, E. A., and L. D. Slater (2009), Biogeophysics: A new frontier in Earth science research, *Rev. Geophys.*, *47*, RG4004, doi:10.1029/2009RG000285.
- Atekwana, E. A., E. A. Atekwana, D. D. Werkema, J. P. Allen, L. A. Smart, J. W. Duris, D. P. Cassidy, W. A. Sauck, and S. Rossbach (2004a), Evidence for microbial enhanced electrical conductivity in hydrocarbon-contaminated sediments, *Geophys. Res. Lett.*, *31*, L23501, doi:10.1029/2004GL021359.
- Atekwana, E. A., D. D. Werkema Jr., J. W. Duris, S. Rossbach, E. A. Atekwana, W. A. Sauck, D. P. Cassidy, J. Means, and F. D. Legall (2004b), In-situ apparent conductivity measurements and microbial population distribution at a hydrocarbon-contaminated site, *Geophysics*, *69*(1), 56–63, doi:10.1190/1.1649375.
- Barrett, T. J., G. M. Anderson, and J. Lugowski (1988), The solubility of hydrogen sulphide in 0–5 m NaCl solutions at 25°–95°C and one atmosphere, *Geochim. Cosmochim. Acta*, *52*(4), 807–811, doi:10.1016/0016-7037(88)90352-3.
- Berner, R. A. (1963), Electrode studies of hydrogen sulfide in marine sediments, *Geochim. Cosmochim. Acta*, *27*(6), 563–575, doi:10.1016/0016-7037(63)90013-9.
- Bigalke, J., and E. W. Grabner (1997), The Geobattery model: A contribution to large scale electrochemistry, *Electrochim. Acta*, *42*(23–24), 3443–3452, doi:10.1016/S0013-4686(97)00053-4.
- Che-Alota, V., E. A. Atekwana, E. A. Atekwana, W. A. Sauck, and D. D. Werkema Jr. (2009), Temporal geophysical signatures from contaminant-mass remediation, *Geophysics*, *74*(4), B113–B123, doi:10.1190/1.3139769.
- Daily, W., and A. Ramirez (1995), Electrical resistance tomography during in-situ trichloroethylene remediation at the Savannah River Site, *J. Appl. Geophys.*, *33*(4), 239–249.
- Davis, C. A., E. Atekwana, E. Atekwana, L. D. Slater, S. Rossbach, and M. R. Mormile (2006), Microbial growth and biofilm formation in geologic media is detected with complex conductivity measurements, *Geophys. Res. Lett.*, *33*, L18403, doi:10.1029/2006GL027312.
- Hubbard, S. S., K. Williams, M. E. Conrad, B. Faybishenko, J. Peterson, J. Chen, P. Long, and T. Hazen (2008), Geophysical monitoring of hydrological and biogeochemical transformations associated with Cr (VI) bioremediation, *Environ. Sci. Technol.*, *42*(10), 3757–3765, doi:10.1021/es071702s.
- Jeroschewski, P., K. Haase, A. Trommer, and P. Gründler (1993), Galvanic sensor for the determination of hydrogen sulphide/sulphide in aqueous media, *Fresenius J. Anal. Chem.*, *346*(10–11), 930–933, doi:10.1007/BF00322753.
- Jeroschewski, P., C. Steuckart, and M. Kühl (1996), An amperometric micro-sensor for the determination of H<sub>2</sub>S in aquatic environments, *Anal. Chem.*, *68*(24), 4351–4357, doi:10.1021/ac960091b.
- Kühl, M., and B. B. Jørgensen (1992), Microsensor measurements of sulfate reduction and sulfide oxidation in compact microbial communities of aerobic biofilms, *Appl. Environ. Microbiol.*, *58*(4), 1164–1174.
- Lawrence, N. S., J. Davis, and R. G. Compton (2000), Analytical strategies for the detection of sulfide: A review, *Talanta*, *52*(5), 771–784, doi:10.1016/S0039-9140(00)00421-5.
- Ledin, M., and K. Pedersen (1996), The environmental impact of mine wastes—Roles of microorganisms and their significance in treatment of mine wastes, *Earth Sci. Rev.*, *41*(1–2), 67–108, doi:10.1016/0012-8252(96)00016-5.
- Linde, N., A. Revil, A. Bolève, C. Dagès, J. Castermant, B. Suski, and M. Voltz (2007), Estimation of the water table throughout a catchment using self-potential and piezometric data in a Bayesian framework, *J. Hydrol.*, *334*(1–2), 88–98, doi:10.1016/j.jhydrol.2006.09.027.
- Luther, G. W., III, T. F. Rozan, M. Taillefer, D. B. Nuzzio, C. Di Meo, T. M. Shank, R. A. Lutz, and S. C. Cary (2001), Chemical speciation drives hydrothermal vent ecology, *Nature*, *410*(6830), 813–816, doi:10.1038/35071069.
- Maier, R. M., I. L. Pepper, and C. P. Gerba (2000), *Environmental Microbiology*, Academic, San Diego, Calif.
- Minsley, B. J., J. Sogade, and F. D. Morgan (2007), Three-dimensional self-potential inversion for subsurface DNAPL contaminant detection at the Savannah River Site, South Carolina, *Water Resour. Res.*, *43*, W04429, doi:10.1029/2005WR003996.
- Mirra, A. (1971), Sulfide analysis by the silver sulfide-silver electrode: Properties of the electrode, *Fresenius, Z. Anal. Chem.*, *254*(2), 114–116, doi:10.1007/BF01166126.
- Naudet, V., A. Revil, J.-Y. Bottero, and P. Bégassat (2003), Relationship between self-potential (SP) signals and redox conditions in contaminated groundwater, *Geophys. Res. Lett.*, *30*(21), 2091, doi:10.1029/2003GL018096.
- Naudet, V., A. Revil, E. Rizzo, J.-Y. Bottero, and P. Bégassat (2004), Groundwater redox conditions and conductivity in a contaminant plume from geoelectrical investigations, *Hydrol. Earth Syst. Sci.*, *8*(1), 8–22, doi:10.5194/hess-8-8-2004.
- Ntarlagiannis, D., and A. Ferguson (2009), SIP response of artificial biofilms, *Geophysics*, *74*(1), A1–A5, doi:10.1190/1.3031514.
- Ntarlagiannis, D., N. Yee, and L. Slater (2005a), On the low-frequency electrical polarization of bacterial cells in sands, *Geophys. Res. Lett.*, *32*, L24402, doi:10.1029/2005GL024751.
- Ntarlagiannis, D., K. H. Williams, L. Slater, and S. Hubbard (2005b), Low-frequency electrical response to microbial induced sulfide precipitation, *J. Geophys. Res.*, *110*, G02009, doi:10.1029/2005JG000024.

- Ntarlagiannis, D., E. A. Atekwana, E. A. Hill, and Y. Gorby (2007), Microbial nanowires: Is the subsurface "hardwired"?, *Geophys. Res. Lett.*, *34*, L17305, doi:10.1029/2007GL030426.
- Nyquist, J. E., and C. E. Corry (2002), Tutorial—Self-potential: The ugly duckling of environmental geophysics, *Leading Edge*, *21*, 446–451, doi:10.1190/1.1481251.
- Personna, Y. R., D. Ntarlagiannis, L. Slater, N. Yee, M. O'Brien, and S. Hubbard (2008), Spectral induced polarization and electrodic potential monitoring of microbially mediated iron sulfide transformations, *J. Geophys. Res.*, *113*, G02020, doi:10.1029/2007JG000614.
- Prodan, C., F. Mayo, J. R. Claycomb, and J. H. Miller (2004), Low-frequency, low-field dielectric spectroscopy of living cell suspensions, *J. Appl. Phys.*, *95*(7), 3754–3756, doi:10.1063/1.1649455.
- Ramsing, N. B., M. Kühl, and B. B. Jørgensen (1993), Distribution of sulfate-reducing bacteria, O<sub>2</sub>, and H<sub>2</sub>S in photosynthetic biofilms determined by oligonucleotide probes and microelectrodes, *Appl. Environ. Microbiol.*, *59*(11), 3840–3849.
- Revil, A., D. Hermitte, M. Voltz, R. Moussa, J.-G. Lacas, G. Bourrié, and F. Trolard (2002), Self-potential signals associated with variations of the hydraulic head during an infiltration experiment, *Geophys. Res. Lett.*, *29*(7), 1106, doi:10.1029/2001GL014294.
- Revsbech, N. P., B. B. Jørgensen, T. H. Blackburn, and Y. Cohen (1983), Microelectrode studies of the photosynthesis and O<sub>2</sub>, H<sub>2</sub>S, and pH profiles of a microbial mat, *Limnol. Oceanogr.*, *28*(6), 1062–1074, doi:10.4319/lo.1983.28.6.1062.
- Revsbech, N. P., B. Madsen, and B. B. Jørgensen (1986), Oxygen production and consumption in sediments determined at high spatial resolution by computer simulation of oxygen microelectrode data, *Limnol. Oceanogr.*, *31*(2), 293–304, doi:10.4319/lo.1986.31.2.0293.
- Rizzo, E., B. Suski, A. Revil, S. Straface, and S. Troisi (2004), Self-potential signals associated with pumping tests experiments, *J. Geophys. Res.*, *109*, B10203, doi:10.1029/2004JB003049.
- Sato, M., and H. M. Mooney (1960), The electrochemical mechanism of sulfide self-potentials, *Geophysics*, *25*(1), 226–249, doi:10.1190/1.1438689.
- Slater, L. D., and D. Lesmes (2002), IP interpretation in environmental investigations, *Geophysics*, *67*(1), 77–88, doi:10.1190/1.1451353.
- Slater, L., D. Ntarlagiannis, N. Yee, M. O'Brien, C. Zhang, and K. H. Williams (2008), Electrode voltages in the presence of dissolved sulfide: Implications for monitoring natural microbial activity, *Geophysics*, *73*(2), F65–F70, doi:10.1190/1.2828977.
- Slater, L. D., F. D. Day-Lewis, D. Ntarlagiannis, M. O'Brien, and N. Yee (2009), Geoelectrical measurement and modeling of biogeochemical breakthrough behavior during microbial activity, *Geophys. Res. Lett.*, *36*, L14402, doi:10.1029/2009GL038695.
- Stumm, W., and J. J. Morgran (1996), *Aquatic Chemistry, Chemical Equilibria and Rates in Natural Waters*, 3rd ed., John Wiley, New York.
- Taillefert, M., G. W. Luther III, and D. B. Nuzzio (2000), The application of electrochemical tools for in situ measurements in aquatic systems, *Electroanalysis*, *12*(6), 401–412, doi:10.1002/(SICI)1521-4109(20000401)12:6<401::AID-ELAN401>3.0.CO;2-U.
- Viollier, E., et al. (2003), Benthic biogeochemistry: State of the art technologies and guidelines for the future of in situ survey, *J. Exp. Mar. Biol. Ecol.*, *285–286*, 5–31, doi:10.1016/S0022-0981(02)00517-8.
- Werkema, D. D., Jr., E. A. Atekwana, A. L. Endres, W. A. Sauck, and D. P. Cassidy (2003), Investigating the geoelectrical response of hydrocarbon contamination undergoing biodegradation, *Geophys. Res. Lett.*, *30*(12), 1647, doi:10.1029/2003GL017346.
- Whitfield, M. (1971), A compact potentiometric sensor of novel design: In situ determination of pH, pS<sup>2-</sup>, and Eh, *Limnol. Oceanogr.*, *16*(5), 829–837, doi:10.4319/lo.1971.16.5.0829.
- Williams, K. H., D. Ntarlagiannis, L. D. Slater, A. Dohnalkova, S. S. Hubbard, and J. F. Banfield (2005), Geophysical imaging of stimulated microbial biomineralization, *Environ. Sci. Technol.*, *39*(19), 7592–7600, doi:10.1021/es0504035.
- Williams, K. H., S. S. Hubbard, and J. F. Banfield (2007), Galvanic interpretation of self-potential signals associated with microbial sulfate-reduction, *J. Geophys. Res.*, *112*, G03019, doi:10.1029/2007JG000440.
- Williams, K. H., A. Kemna, M. J. Wilkins, J. Druhan, E. Arntzen, A. L. N'Guessan, P. E. Long, S. S. Hubbard, and J. F. Banfield (2009), Geophysical monitoring of coupled microbial and geochemical processes during stimulated subsurface bioremediation, *Environ. Sci. Technol.*, *43*(17), 6717–6723, doi:10.1021/es900855j.

R. Doherty, Environmental Engineering Research Centre, School of Planning, Architecture and Civil Engineering, Queen's University of Belfast, Belfast BT9 5AG, UK.

D. Ntarlagiannis, L. Slater, and C. Zhang, Department of Earth and Environmental Sciences, Rutgers, State University of New Jersey, Newark, NJ 07102, USA. (chizhang@pegasus.rutgers.edu)